

Reaction Systems Related to Dissimilatory Nitrate Reductase: Nitrate Reduction Mediated by Bis(dithiolene)tungsten Complexes

Jianfeng Jiang and R. H. Holm*

Department of Chemistry and Chemical Biology, Harvard University,
Cambridge, Massachusetts 02138

Received September 15, 2004

Kinetics of the oxygen atom transfer reactions $[M^{IV}(QC_6H_2-2,4,6-Pr'_3)(S_2C_2Me_2)_2]^{1-} + XO \rightarrow [M^{VI}O(QC_6H_2-2,4,6-Pr'_3)(S_2C_2Me_2)_2]^{1-} + X$ in acetonitrile with substrates $XO = NO_3^-$ and $(CH_2)_4SO$ have been determined. The reactants are bis(dithiolene) complexes with $M = Mo, W$ and sterically encumbered axial ligands with $Q = O, S$ to stabilize mononuclear square pyramidal structures. The complex $[Mo^{IV}(SC_6H_2-2,4,6-Pr'_3)(S_2C_2Me_2)_2]^{1-}$ is an analogue of the active site of dissimilatory nitrate reductase which in the reduced state contains a molybdenum atom bound by two pyranopterindithiolene ligands and a cysteinyl residue. Nitrate reduction was studied with tungsten complexes because of unfavorable stability properties of the molybdenum complexes. Product nitrite was detected by a colorimetric method. All reactions with both substrates are second-order with associative transition states ($\Delta S^\ddagger \sim -20$ eu). Variation of atoms M and Q , together with data from prior work, allows certain kinetics comparisons to be made. Among them, $k_2^W/k_2^{Mo} = 25$ for $(CH_2)_4SO$ reduction ($Q = S$), an expression of the kinetic metal effect. Further, $k_2^S/k_2^O = 28$ and $\sim 10^4$ for nitrate and $(CH_2)_4SO$ reduction, respectively, effects attributed to relatively more steric congestion in achieving the transition state with hindered phenolate vs thiolate ligands. The effect is more pronounced with the larger substrate. These results demonstrate the feasibility of tungsten-mediated nitrate reduction by direct atom transfer using molecules with both axial thiolate and phenolate ligands. Complexes of the type $[M^{IV}(OR)(S_2C_2Me_2)_2]$ are capable of reducing biological N -oxide, S -oxide, and nitrate substrates and thus constitute functional analogue reaction systems of enzymic transformations.

Introduction

In elaborating bioinorganic aspects of molybdenum and tungsten chemistry,^{1–4} we have utilized ene-1,2-dithiolates as structural and electronic simulants of the pyranopterindithiolene cofactor ligand (S_2pd) in Figure 1. This research has afforded, among other complexes, square pyramidal desoxo $[M^{IV}(OR)(S_2C_2Me_2)_2]^{1-}$ ($M = Mo, W$) and distorted octahedral monooxo $[W^{VI}O(OR)(S_2C_2Me_2)_2]^{1-}$. The molybdenum complexes are analogues of the reduced sites of the DMSOR family under the Hille classification.^{5,6} Using the minimal reaction paradigm $M^{IV} + XO \rightarrow M^{VI}O + X$, functional analogue systems have been developed which reduce the biological substrates $XO = Me_3NO$ and Me_2SO

(and others) in second-order reactions that proceed through an associative transition state.^{7,8} Leading aspects of this research are summarized elsewhere.⁴

The scope of atom transfer reactions mediated by the foregoing molybdenum and tungsten complexes with both biological and abiological substrates is a matter of continuing interest. Very recently, we have demonstrated related molybdenum- and tungsten-mediated bimolecular sulfur atom transfer reactions.⁹ In addition to DMSOR and trimethylamine N -oxide reductase, the DMSOR family includes dissimilatory nitrate reductase.⁵ These enzymes catalyze reaction 1 and are found in certain bacteria that have the ability to grow on nitrate and reduce it for respiration. The structure of NiR from *Desulfovibrio desulfuricans* has been solved at 1.9 Å resolution.¹⁰ The oxidized active site is revealed as $[Mo^{VI}(OH/OH_2)(S \cdot Cys)(S_2pd)_2]$, and the desoxo

- (1) Holm, R. H. *Coord. Chem. Rev.* **1990**, *100*, 183–221.
- (2) Enemark, J. H.; Young, C. G. *Adv. Inorg. Chem.* **1994**, *40*, 1–88.
- (3) McMaster, J.; Tunney, J. T.; Garner, C. D. *Prog. Inorg. Chem.* **2004**, *52*, 539–583.
- (4) Enemark, J. H.; Cooney, J. J. A.; Wang, J.-J.; Holm, R. H. *Chem. Rev.* **2004**, *104*, 1175–1200.
- (5) Hille, R. *Chem. Rev.* **1996**, *96*, 2757–2816.
- (6) Abbreviations are given in Chart 1.

- (7) Lim, B. S.; Holm, R. H. *J. Am. Chem. Soc.* **2001**, *123*, 1920–1930.
- (8) Sung, K.-M.; Holm, R. H. *J. Am. Chem. Soc.* **2001**, *123*, 1931–1943.
- (9) Wang, J.-J.; Kryatova, O.; Rybak-Akimova, E. V.; Holm, R. H. *Inorg. Chem.* **2004**, *43*, 8092.

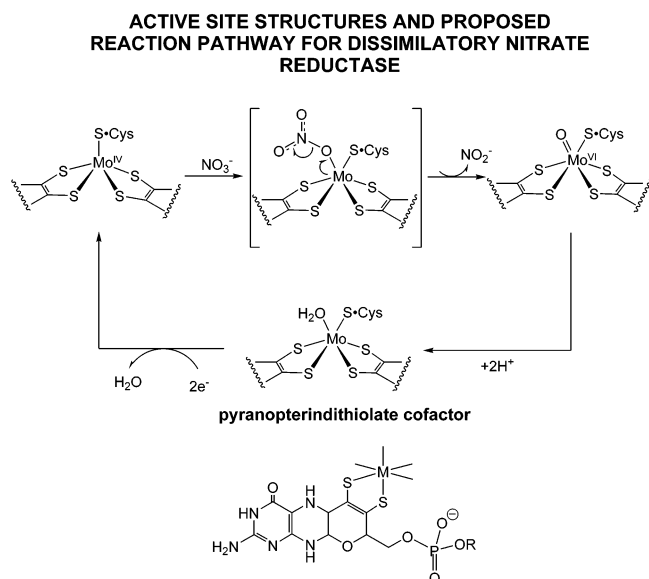
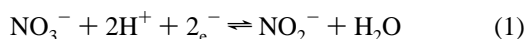


Figure 1. Schematic depictions of the reduced and oxidized sites of dissimilatory nitrate reductase (*Desulfovibrio desulfuricans*) and the proposed reaction pathway. Also shown is the pyranopterindithiolate cofactor (R absent or a nucleotide).

site $[\text{Mo}^{\text{IV}}(\text{S}\cdot\text{Cys})(\text{S}_2\text{pd})_2]$ has been proposed to intervene in catalysis. The situation is set out in Figure 1, where the



oxidized site is presented in the deprotonated (oxo) form accessible in synthetic complexes. The structure of a second dissimilatory enzyme has been crystallographically established. NiR A from *Escherichia coli* contains a $[\text{Mo}(\text{O}_2\text{-C}\cdot\text{Asp})(\text{S}_2\text{pd})_2]$ site with an unsymmetrically coordinated carboxylate group.¹¹ These sites bind *two* pyranopterindithiolene ligands, one of the defining features of the DMSOR family, but differ in the protein-based ligand between each other and with other members of the family. In DMSOR and TMAOR,^{12,13} the oxidized (deprotonated) site is $[\text{Mo}^{\text{VI}}\text{O}(\text{O}\cdot\text{Ser})(\text{S}_2\text{pd})_2]$, devoid of cysteinyl or carboxylate ligation.

With the availability by synthesis of the reactant complexes $[\text{M}^{\text{IV}}(\text{SR})(\text{S}_2\text{C}_2\text{Me}_2)_2]^{1-}$ ($\text{M} = \text{Mo},^{7,14} \text{W}^{15}$) and their oxidation products $[\text{W}^{\text{VI}}\text{O}(\text{SR})(\text{S}_2\text{C}_2\text{Me}_2)_2]^{1-}$,¹⁵ an examination of nitrate reduction by oxygen atom transfer in analogue reaction systems with thiolate ligation becomes feasible. In addition, the reactant complexes $[\text{M}^{\text{IV}}(\text{OR})(\text{S}_2\text{C}_2\text{Me}_2)_2]^{1-}$ ($\text{M} = \text{Mo},^{14} \text{W}^{16}$) and $[\text{W}^{\text{VI}}\text{O}(\text{OR})(\text{S}_2\text{C}_2\text{Me}_2)_2]^{1-}$ ⁸ admit examination of the effect of sulfur vs oxygen axial ligation

on the kinetics of nitrate reduction. Although we are unaware of any tungsten-containing NiR, we utilize tungsten because of its generally better stability in reducing ligand environments such as that in bis(dithiolene) complexes. Further, in this and much of our past work we have attempted to develop molybdenum and tungsten dithiolene chemistry in parallel, the principal motivation being the existence of Mo/W isoenzymes.¹⁷

Experimental Section

Preparation of Compounds. All reactions and manipulations were performed under a pure dinitrogen atmosphere using either modified Schlenk techniques or an inert atmosphere box. Solvents were passed through an Innovative Technology solvent purification system prior to use. Tetramethylenesulfoxide ($(\text{CH}_2)_4\text{SO}$) was vacuum-distilled before use. $(\text{Bu}_4\text{N})(\text{NO}_3)$ was a commercial sample (Aldrich) and was used as received. $(\text{Et}_4\text{N})(\text{NO}_2)^{18}$ was recrystallized from acetonitrile/ether. The compounds $(\text{Et}_4\text{N})(\text{SC}_6\text{H}_2\text{-2,4,6-Pr}_3)$ and $(\text{Et}_4\text{N})(\text{OC}_6\text{H}_2\text{-2,4,6-Pr}_3)$ were prepared from equimolar $\text{HSC}_6\text{H}_2\text{-2,4,6-Pr}_3^{19}$ or $\text{HOC}_6\text{H}_2\text{-2,4,6-Pr}_3^{14}$ with 25% Et_4NOH in methanol and were isolated as colorless crystalline solids from acetonitrile/ether. The compounds $(\text{Et}_4\text{N})[\text{M}(\text{SC}_6\text{H}_2\text{-2,4,6-Pr}_3)(\text{S}_2\text{C}_2\text{-Me}_2)_2]$ ($\text{M} = \text{Mo},^{14} \text{W}^{15}$) were prepared as described.

$(\text{Et}_4\text{N})[\text{Mo}(\text{OC}_6\text{H}_2\text{-2,4,6-Pr}_3)(\text{S}_2\text{C}_2\text{Me}_2)_2]$. To a suspension of 72 mg (0.19 mmol) of $[\text{Mo}(\text{CO})_2(\text{S}_2\text{C}_2\text{Me}_2)_2]^{20}$ in 2 mL of acetonitrile was added a solution of 65 mg (0.19 mmol) $(\text{Et}_4\text{N})\text{-(OC}_6\text{H}_2\text{-2,4,6-Pr}_3)$ in 1 mL of acetonitrile. The mixture was stirred for 15 h to give a red-brown solution which was filtered through Celite. The solvent was removed. The residue was washed with ether (3×15 mL) and extracted with 1 mL of 1:4 (v/v) acetonitrile/THF; the extract was covered with 60 mL of ether. A red-brown crystalline solid appeared upon allowing the mixture to stand for 3 d. The solid was collected, washed with ether (3×5 mL), and dried to afford the product as 69 mg (54%) of a brown microcrystalline solid. Absorption spectrum (acetonitrile): λ_{max} (ϵ_{M}) 331 (13000), 415 (4000), 570 (580), 729 (150) nm. ^1H NMR (CD_3CN , anion): δ 1.04 (d, 12), 1.14 (d, 6), 2.53 (s, 12), 2.88 (m, 1), 3.24 (m, 2), 6.65 (s, 2).

$(\text{Et}_4\text{N})[\text{W}(\text{OC}_6\text{H}_2\text{-2,4,6-Pr}_3)(\text{S}_2\text{C}_2\text{Me}_2)_2]$. To a suspension of 112 mg (0.24 mmol) of $[\text{W}(\text{CO})_2(\text{S}_2\text{C}_2\text{Me}_2)_2]^{20}$ in 2 mL of acetonitrile was added a solution of 82 mg (0.24 mmol) $(\text{Et}_4\text{N})\text{-(OC}_6\text{H}_2\text{-2,4,6-Pr}_3)$ in 1 mL of acetonitrile. The mixture became green-brown immediately with accompanying gas evolution. Solvent was removed after stirring for 2 h. The residue was washed with ether (3×15 mL) and extracted with 2 mL of 1:4 (v/v) acetonitrile/THF; the extract was covered with 60 mL of ether. Crystalline solid appeared after allowing the mixture to stand for 1 d. The solid was collected, washed with ether (3×5 mL), and dried to afford the product as 79 mg (44%) of a green-brown microcrystalline solid. Absorption spectrum (acetonitrile): λ_{max} (ϵ_{M}) 295 (15000), 319 (sh, 11000), 355 (5700), 394 (sh, 2400), 464 (950), 530 (200) nm. ^1H NMR (CD_3CN , anion): δ 1.00 (d, 12), 1.11 (d, 6), 2.56 (s, 12), 2.80 (m, 1), 3.19 (m, 2), 6.71 (s, 2).

$(\text{Et}_4\text{N})[\text{W}(\text{OC}_6\text{H}_2\text{-2,4,6-Pr}_3)(\text{S}_2\text{C}_2\text{Me}_2)_2]$. To a solution of 49 mg (0.062 mmol) of $(\text{Et}_4\text{N})[\text{W}(\text{OC}_6\text{H}_2\text{-2,4,6-Pr}_3)(\text{S}_2\text{C}_2\text{Me}_2)_2]$ in 1

- (10) Dias, J. M.; Than, M. E.; Humm, A.; Huber, R.; Bourenkov, G. P.; Bartunik, H. D.; Bursakov, S.; Calvete, J.; Caldeira, J.; Carneiro, C.; Moura, J. J. G.; Moura, I.; Romão, M. J. *Structure* **1999**, 7, 65–79.
- (11) Bertero, M. G.; Rothery, R. A.; Palak, M.; Hou, C.; Lim, D.; Blasco, F.; Weiner, J. H.; Strynadka, N. C. J. *Nature Struct. Biol.* **2003**, 10, 681–687.
- (12) Li, H.-K.; Temple, C.; Rajagopalan, K. V.; Schindelin, H. *J. Am. Chem. Soc.* **2000**, 122, 7673–7680.
- (13) Czjzek, M.; Dos Santos, J.-P.; Pommier, J.; Méjean, V.; Haser, R. *J. Mol. Biol.* **1998**, 284, 435–447.
- (14) Lim, B. S.; Donahue, J. P.; Holm, R. H. *Inorg. Chem.* **2000**, 39, 263–273.
- (15) Jiang, J.; Holm, R. H. *Inorg. Chem.* **2004**, 43, 1302–1310.
- (16) Sung, K.-M.; Holm, R. H. *Inorg. Chem.* **2000**, 39, 1275–1281.

- (17) Garner, C. D.; Stewart, L. J. *Met. Ions Biol. Syst.* **2002**, 39, 699–726.
- (18) Hyde, M. R.; Garner, C. D. *J. Chem. Soc., Dalton Trans.* **1975**, 1186–1191.
- (19) Blower, P. J.; Dilworth, J. R.; Hutchinson, J. P.; Zubieta, J. A. *J. Chem. Soc., Dalton Trans.* **1985**, 1533–1541.
- (20) Fomichev, D. V.; Lim, B. S.; Holm, R. H. *Inorg. Chem.* **2001**, 40, 645–654.

Chart 1. Designation of Complexes and Abbreviations

$[\text{Mo}^{\text{IV}}(\text{OPh})(\text{S}_2\text{C}_2\text{Me}_2)_2]^{1-}$	1 ⁷
$[\text{Mo}^{\text{IV}}(\text{OC}_6\text{H}_2\text{-2,4,6-Pr}^i_3)(\text{S}_2\text{C}_2\text{Me}_2)_2]^{1-}$	2
$[\text{Mo}^{\text{IV}}(\text{SC}_6\text{H}_2\text{-2,4,6-Pr}^i_3)(\text{S}_2\text{C}_2\text{Me}_2)_2]^{1-}$	3 ¹⁴
$[\text{W}^{\text{IV}}(\text{OPh})(\text{S}_2\text{C}_2\text{Me}_2)_2]^{1-}$	4 ¹⁶
$[\text{W}^{\text{IV}}(\text{OC}_6\text{H}_2\text{-2,4,6-Pr}^i_3)(\text{S}_2\text{C}_2\text{Me}_2)_2]^{1-}$	5
$[\text{W}^{\text{IV}}(\text{SC}_6\text{H}_2\text{-2,4,6-Pr}^i_3)(\text{S}_2\text{C}_2\text{Me}_2)_2]^{1-}$	6 ¹⁵
$[\text{W}^{\text{VI}}\text{O}(\text{OC}_6\text{H}_2\text{-2,4,6-Pr}^i_3)(\text{S}_2\text{C}_2\text{Me}_2)_2]^{1-}$	7
$[\text{W}^{\text{VI}}\text{O}(\text{SC}_6\text{H}_2\text{-2,4,6-Pr}^i_3)(\text{S}_2\text{C}_2\text{Me}_2)_2]^{1-}$	8 ¹⁵

DMSOR, dimethyl sulfoxide reductase; NiR, nitrate reductase; S₂pd, pyranopterindithiolene(2-) cofactor ligand; TMAOR, trimethylamine oxide reductase

mL of acetonitrile was added a solution of 22 mg (0.066 mmol) of Ph₃AsO in 1 mL of THF. The green-brown solution became dark brown within 2 min; the reaction mixture was stirred for 15 min. Solvent was removed and the residue was rinsed with ether (3 × 3 mL). The residue was extracted with 1 mL of acetonitrile. Ether (50 mL) was added to the extract, and the mixture was maintained at −40 °C for 2 d. The solid that separated was collected, washed with ether (3 × 3 mL), and dried. The product was obtained as 25 mg (50%) of a dark brown microcrystalline solid. Absorption spectrum (acetonitrile): λ_{max} (ε_M) 353 (sh, 6000), 401 (sh, 3300), 533 (1700), 667 (1300) nm. ¹H NMR (CD₃CN anion): δ 1.10 (d, 12), 1.18 (d, 6), 2.20 (s, 12), 6.89 (s, 2), 2.84 (m, 2), 3.80 (m, 1).

In the following sections, complexes are numerically designated according to Chart 1.

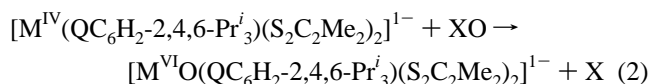
Kinetics Measurements. Procedures and data analysis were performed as in previous kinetics studies.⁷ Sample preparations and reactions were carried out under strictly anaerobic conditions in acetonitrile solutions. Acetonitrile (Burdick & Jackson) was stored over 4-Å molecular sieves for 2 d prior to use. The reaction systems were conventionally monitored with a Varian Cary 3 spectrophotometer equipped with a cell compartment thermostated to ±0.5 K. Thermal equilibrium was reached by placing a quartz cell (1 mm path length) containing a 0.25 mL solution of the substrate in the cell compartment at least 5 min prior to reaction initiation. Reactions were initiated by the injection of complexes using a gastight syringe (100 μL) through the rubber septum cap of the quartz cell followed by rapid shaking of the solution mixtures. The following initial concentrations were used: [6]₀ = 0.20–0.60 mM, [(Bu₄N)(NO₃)]₀ = 4.0–60 mM; [6]₀ = 0.30–0.60 mM, [(CH₂)₄-SO]₀ = 20–800 mM; [5]₀ = 0.30–0.60 mM, [(Bu₄N)(NO₃)]₀ = 90–800 mM; [5]₀ = 0.30–0.60 mM, [(CH₂)₄SO]₀ = 1.9–7.9 M; [3]₀ = 0.30–0.60 mM, [(CH₂)₄SO]₀ = 0.16–4.7 M. Tight isosbestic points were observed in each reaction system, indicating no significant accumulation of an intermediate. For each substrate, reactions were conducted at five different temperatures in the range of 288–338 K. At each temperature, at least five independent runs with different initial substrate concentrations were performed under pseudo-first-order conditions for these complexes. Plots of ln[(A_t − A_∞)/(A₀ − A_∞)] vs time were linear over 3–5 half-lives and the initial rate constants *k*_{obs} were obtained from the data for the first 30 min. Plots of *k*_{obs} vs [substrate]₀ were linear and yielded overall second-order rate constants *k*₂ at each temperature. Activation parameters were determined from linear plots of the Eyring equation *k* = (*k*_B*T*/h)[exp(Δ*S*‡/*R* − Δ*H*‡/*RT*)]. Standard deviations of rate constants were estimated by using linear least-squares error analysis with uniform weighting of data points.

Determination of Nitrite. Nitrite generated in the system was measured quantitatively by a colorimetric method.²¹ After completion of an oxo transfer reaction, the reaction mixture was reduced to dryness and the residue was extracted with 100 mL of water. An aqueous solution of sulfanilamide and *N*-(1-naphthyl)ethylene-diamine dihydrochloride was added to the extract to give a purple solution. The absorbance at 550 nm was measured and the concentration was acquired by comparison with a standard curve measured with NaNO₂. Nitrite generated in the various systems corresponded to 85–95% of the theoretical conversion for a complete reaction.

Other Physical Measurements. All measurements were made under anaerobic conditions. NMR spectra were recorded on Varian Mercury 300 or 400 spectrometers. Absorption spectra were determined with a Varian Cary 3 or Varian Cary 50 spectrophotometer at 298 K.

Results and Discussion

Reaction Systems. Bis(dithiolene)molybdenum and -tungsten complexes with axial phenolate ligands, exemplified by **1** and **4**, have been highly effective in mediating clean and complete oxo and sulfido transfer reactions.^{7–9} However, the corresponding complexes with benzenethiolate or relatively small thiolate or selenolate ligands in general have resisted isolation. Instead, binuclear species such as [Mo^{IV}₂(μ₂-SePh)₂(S₂C₂Ph₂)₄]^{2−}¹⁴ or mononuclear [W^V(QPh)₂(S₂C₂Me₂)₂]^{1−} (Q = S, Se)²² were obtained. However, the use of the sterically demanding substituents R = 2-adamantyl⁷ or 2,4,6-triisopropylphenyl^{14,15} has allowed isolation of the desired complexes [M^{IV}(SR)(S₂C₂Me₂)₂]^{1−}. No attempt has been made to determine the smallest R group that stabilizes complexes of this formulation. To augment complexes of the hindered phenolate type, **2** and **5** were prepared in this work. The ability of sterically crowded complexes to sustain oxo transfer is demonstrated by reaction 2 (M = W) with XO/X = Ph₃-AsO/Ph₃As, in which **5** (Q = O) is converted to **7** (50%) and **6** (Q = S) to **8** (68%)¹⁵ in the indicated isolated yields. The complexes [Mo^{IV}(OR)(S₂C₂Me₂)₂]^{1−} support oxo transfer with *N*-oxides and *S*-oxides, but in no case has the reaction product been sufficiently stable for isolation. As shown in a detailed study of the reactions of phenolate complex **1**, species of the type [Mo^{VI}O(OR)(S₂C₂Me₂)₂]^{1−} undergo an internal redox reaction to afford the products [Mo^{VO}(S₂-C₂Me₂)₂]^{1−} and RO•, which is quenched to form ROH.⁷



The kinetics of reaction 2, which is set out schematically in Figure 2, have been established. The square pyramidal stereochemistry of the reactants is based on the structures of **1**,⁷ **3**,¹⁴ **4**,¹⁶ **6**,¹⁵ and [Mo^{IV}(OC₆H₃-2,6-Pr^{*i*}₂)(S₂C₂Me₂)₂]^{1−}.¹⁴ The metal atom is situated 0.78–0.83 Å (M–OR) or 0.70–0.73 Å (M–SR) above the equatorial S₄ plane toward the axial ligand. Other parameters are M–OR = 1.86–1.90 Å,

(21) Basset, J.; Denney, R. C.; Jeffery, G. H.; Mendham, J. In *Vogel's Textbook of Quantitative Chemical Analysis*; Longman Scientific and Technical: 1989; pp 702 ff.

(22) Sung, K.-M.; Holm, R. H. *Inorg. Chem.* **2001**, *40*, 4518–4525.

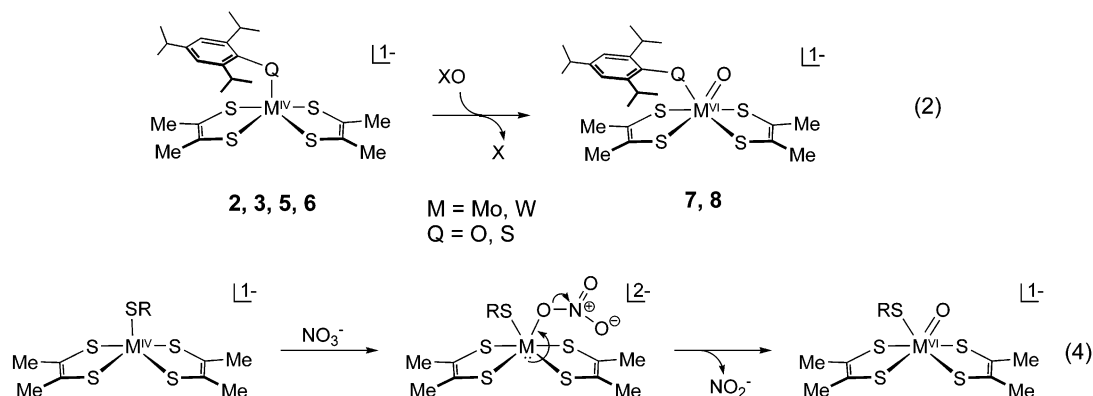


Figure 2. Upper: schematic representation of oxygen atom transfer reactions of Mo^{IV} (**2**, **3**) and W^{IV} (**5**, **6**) complexes with sterically hindered phenolate or thiolate axial ligands containing the 2,4,6-triisopropylphenyl substituent. The Mo^{VIO} product complexes are too unstable to be isolated whereas the W^{VIO} complexes (**7**, **8**) are isolable. Lower: associative reaction pathway for nitrate reduction.

Table 1. Kinetics Parameters for the Oxygen Atom Transfer Reaction Systems $[\text{M}^{\text{IV}}(\text{QR})(\text{S}_2\text{C}_2\text{Me}_2)_2]/\text{XO}$ in Acetonitrile

M	QR	XO	k_2 ($\text{M}^{-1} \text{s}^{-1}$) ^a	ΔH^\ddagger (kcal/mol)	ΔS^\ddagger (eu)
Mo ^b	OPh	$(\text{CH}_2)_4\text{SO}^d$	$1.5(2) \times 10^{-4}$	10.1(4)	−39(1)
Mo	$\text{SC}_6\text{H}_2\text{Pr}_3$	$(\text{CH}_2)_4\text{SO}^e$	$1.4(1) \times 10^{-3}$	16.8(6)	−16(2)
W ^c	OPh	$(\text{CH}_2)_4\text{SO}^d$	$9.0(3) \times 10^{-4}$	11.6(4)	−33(1)
W	$\text{OC}_6\text{H}_2\text{Pr}_3$	$(\text{CH}_2)_4\text{SO}^g$	$2.3(1) \times 10^{-6}$	18.6(7)	−22(2)
W	$\text{OC}_6\text{H}_2\text{Pr}_3$	NO_3^- ^f	$6.1(1) \times 10^{-3}$	15.8(4)	−16(1)
W	$\text{SC}_6\text{H}_2\text{Pr}_3$	$(\text{CH}_2)_4\text{SO}^{e,g}$	$3.5(1) \times 10^{-2}$	14.6(9)	−16(3)
W	$\text{SC}_6\text{H}_2\text{Pr}_3$	NO_3^- ^f	$1.7(1) \times 10^{-1}$	12.6(9)	−20(3)

^a Measured values at 298 K. ^b Reference 7. ^c Reference 8. ^d $k_2^{\text{W}}/k_2^{\text{Mo}} = 6.0$. ^e $k_2^{\text{W}}/k_2^{\text{Mo}} = 25$. ^f $k_2^{\text{S}}/k_2^{\text{O}} = 28$. ^g $k_2^{\text{S}}/k_2^{\text{O}} = 10^4$.

$\text{M}-\text{SR} = 2.32\text{--}2.34 \text{ \AA}$, $\text{M}-\text{O}-\text{C} = 135, 147^\circ$ (**1**, **4**), 167° , ¹⁴ and $\text{M}-\text{S}-\text{C} = 102\text{--}104^\circ$ (**3**, **6**). In the phenolate series, the presence of Pr^i groups on ring increase the $\text{Mo}-\text{O}-\text{C}$ angle by 32° ; bond distances are not significantly affected by the larger axial ligands. The distorted octahedral product configuration is demonstrated by the structures of $[\text{W}^{\text{VIO}}(\text{O}(\text{Ph})(\text{S}_2\text{C}_2\text{Me}_2)_2)]^{1-}$ **8** and **7**.¹⁵ These structures are metrically very similar except for the 0.44 \AA difference in $\text{W}-\text{QR}$ bond lengths.

Initial observations revealed that the molybdenum complexes **2** and **3** are inadmissible for examination of nitrate reduction. Phenolate complex **2** showed an extremely sluggish reaction with excess nitrate in acetonitrile. Reaction systems containing thiolate complex **3** and excess nitrate in both acetonitrile and DMF solutions were not well-behaved. The complex underwent decomposition to $[\text{Mo}(\text{S}_2\text{C}_2\text{Me}_2)_3]^{1-}$,²⁰ identified spectrophotometrically, at rates much faster than oxo transfer. However, an intrinsic ability of **3** to support oxo transfer was demonstrated by the clean reduction of $(\text{CH}_2)_4\text{SO}$ to $(\text{CH}_2)_4\text{S}$; kinetics data are contained in Table 1. With the finding that complexes of the native metal of dissimilatory NiR are unsuitable, attention was directed to the tungsten-based systems in reaction 2 with **5** or **6** and $\text{XO}/\text{X} = \text{NO}_3^-/\text{NO}_2^-$. To provide controls and a comparative rate basis, reduction of the well-studied substrate $\text{X} = (\text{CH}_2)_4\text{SO}$,^{7,8} the least hindered *S*-oxide, was examined in parallel with nitrate reduction. In reaction systems involving **5** and **6** and 5–10 equiv of nitrite, it was observed that a rapid color change from red-brown to purple ensued. Equimolar quantities of the complexes and nitrite gave a slower reaction; the ^1H NMR and UV/visible spectra of the reaction showed

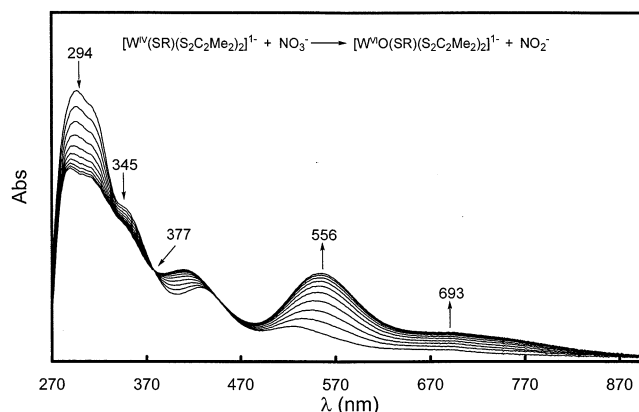


Figure 3. UV/visible spectra for the specified reaction ($\text{R} = \text{C}_6\text{H}_2\text{-}2,4,6\text{-Pr}_3$) in acetonitrile at room temperature; band maxima and an isosbestic point are indicated. The system contained $[\text{6}]_0 = 0.22 \text{ mM}$ and $[(\text{Bu}_4\text{N})\text{-(NO}_3\text{)}]_0 = 26.2 \text{ mM}$; spectra were recorded every 50 s.

that the product in these systems was not oxo complex **7** or **8**. A limited kinetics study indicated that the rate constants of these reactions were ca. 5–10 times larger than that for nitrate reduction (see below). Consequently, the reactions **2** were performed with, usually, 50 equiv or more of nitrate. Under these pseudo-first-order conditions, well-behaved kinetics were observed.

Substrate Reduction Kinetics. Addition of ca. 100 equiv of nitrate to an acetonitrile solution of **6** resulted in a gradual color change from red-brown to purple. Spectral changes are shown in Figure 3. The intense features at 294 and 345 nm decrease with time; the final spectrum with $\lambda_{\text{max}} = 556$ and 693 nm is identical to that of complex **8** measured separately. Note the tight isosbestic point at 377 nm. In this and other nitrate reduction reactions, 85–95% of nitrite expected from stoichiometric conversion was detected by a colorimetric method. Reduction of $\text{XO} = \text{NO}_3^-$ and $(\text{CH}_2)_4\text{SO}$ by **5** and **6** were found to produce tight isosbestic points and final spectra which are those of **7** and **8**, respectively, and to obey the second-order rate law 3, a consistent feature of all substrate transformations mediated by bis(dithiolene)molybdenum and -tungsten complexes.^{7–9} The parameters collected

$$-\text{d}[\text{M}^{\text{IV}}]/\text{d}t = k_2[\text{M}^{\text{IV}}][\text{XO}] \quad (3)$$

in Table 1 allow several kinetics comparisons and other features to be examined.

(i) Steric Effects. The rate constant ratio $k_2(\mathbf{4})/k_2(\mathbf{5}) \approx 400$ signifies a moderate rate retardation in the reaction of unhindered vs hindered W^{IV} phenolate complexes with the same substrate. This factor is likely to be substrate-dependent (not tested).

(ii) Kinetic Metal Effect. The ratios $k_2^{\text{W}}(\mathbf{4})/k_2^{\text{Mo}}(\mathbf{1}) = 6^8$ and $k_2^{\text{W}}(\mathbf{6})/k_2^{\text{Mo}}(\mathbf{2}) = 25$ are another manifestation of oxo transfer from substrate to metal being faster with tungsten than molybdenum. The rate discrimination for these reactions, which implicate $\text{M}^{\text{IV}} \rightarrow \text{M}^{\text{VI}}$ oxidation, is not large, ratios typically being $\lesssim 50$. We have encountered no exceptions to this behavior, which we take as a periodic property. Rate constant data and discussion of this behavior are available elsewhere.^{4,8,23} Isoelectronic molybdenum and tungsten complexes with identical ligation are isostructural and nearly isodimensional and, at least with bis(dithiolenes), follow the same rate law at constant substrate. Consequently, a practical utility of the kinetic metal effect is definition of reaction pathways of molybdenum systems of insufficient robustness with use of analogous, more stable tungsten systems which can deliver all necessary information except exact rate constants. Note, however, that for substrate reductions these values are likely to agree within 2 orders of magnitude. The present study of nitrate reduction offers an application of the kinetic metal effect, which is also manifested by molybdenum and tungsten isoenzymes.⁴

(iii) Sulfur vs Oxygen Axial Ligands. The ratio $k_2^{\text{S}}(\mathbf{6})/k_2^{\text{O}}(\mathbf{5}) = 28$ reveals that nitrate is reduced faster at a W–SR vs a W–OR site at constant $\text{R} = \text{C}_6\text{H}_2\text{-2,4,6-Pr}_3$ and dithiolene ligands. A much greater discrimination factor of $\sim 10^4$ is found with the same complexes and $(\text{CH}_2)_4\text{SO}$ as substrate. The first result implies that an enzymic site with W–S·Cys binding is a more effective catalyst than a W–O·Ser site in the absence of protein environmental effects. The kinetic metal effect suggests that the statement can be extrapolated to molybdenum sites. However, this matter cannot be tested at present, as there are no reports of nitrate reduction by other members of the DMSOR family nor of *N*-oxide or *S*-oxide reduction by NiR.

(iv) Reaction Pathway. For all reactions in Table 1, ΔS^\ddagger is negative, consistent with an associative transition state. Values are less negative than for systems based on **1** and **4** with the same substrate, suggesting a less-ordered transition

state possibly arising from less specific solvation owing to the larger axial substituents. For the reactions studied here, ΔH^\ddagger is 68–78% of ΔG^\ddagger and $\Delta H^{\ddagger\text{O}} > \Delta H^{\ddagger\text{S}}$ at constant substrate, although the effect is not large (3–4 kcal/mol). We interpret this to mean that rate differences arise primarily from energy required to bind substrate in the more congested coordination environment afforded by an axial W–OR than W–SR ligand, a matter supported by the W–QR bond distances and W–Q–C bond angles specified above. In this picture, the parameters of the initial square pyramidal configuration, especially the W–QR bond lengths and W–Q–C bond angles (see above), are the dominant factors as the ground-state structure evolves to the transition state geometry by binding substrate cis to the QR ligand, as observed in the product stereochemistry. The much smaller discrimination factor for nitrate reduction by **5** and **6** in (iii) is proposed to arise because of the small planar structure of the substrate, whose binding is less sensitive to steric influences. This factor is ca. 10^3 larger for $(\text{CH}_2)_4\text{SO}$ which, while not a sterically crowded molecule, is evidently large enough to differentiate among different steric environments. Another possible factor is the intrinsic binding propensity of a W–SR vs W–OR site in the absence of steric effects. We find this artificial situation difficult to assess and leave the matter open. Depiction of the pathway of nitrate reduction with axial thiolate ligation is included as reaction 4 in Figure 2.

Last, there are prior examples of molybdenum- and tungsten-mediated nitrate reduction systems.^{24,25} At least one of them was designed to simulate biological nitrate reduction,²⁵ but was executed before the structure of any molybdoenzyme site was known. Nonetheless, the present investigation together with the previous system demonstrates that nitrate reduction by primary (direct) oxo transfer²⁴ is a feasible reaction pathway. Oxygen isotope labeling experiments, possibly designed like those which demonstrated oxo transfer in DMSOR,²⁶ are required to demonstrate primary atom transfer from substrate to molybdenum in NiR.

Acknowledgment. This work was supported by NSF Grant CHE 0237419. We thank Dr. S. C. Lee for useful discussions.

IC040109Y

(23) Tucci, G. C.; Donahue, J. P.; Holm, R. H. *Inorg. Chem.* **1998**, *37*, 1602–1608.

(24) Holm, R. H. *Chem. Rev.* **1987**, *87*, 1401–1449, and references therein.

(25) Craig, J. A.; Holm, R. H. *J. Am. Chem. Soc.* **1989**, *111*, 2111–2115.

(26) Schultz, B. E.; Holm, R. H.; Hille, R. *J. Am. Chem. Soc.* **1995**, *117*, 827–828.